

New acoustic instrumentation for the SIMPLE superheated droplet detector

M. Felizardo^{a,b,c,*}, R.C. Martins^b, A.R. Ramos^{a,c}, T. Morlat^{c,1}, T.A. Girard^c,
F. Giuliani^{c,2}, J.G. Marques^{a,c}

^aInstituto Tecnológico e Nuclear, Estrada Nacional 10, 2686-953 Sacavém, Portugal

^bInstituto de Telecomunicações, IST, Av. Rovisco Pais 1, 1049-001 Lisbon, Portugal

^cCentro de Física Nuclear, Universidade de Lisboa, 1649-003 Lisbon, Portugal

Received 27 December 2007; received in revised form 6 February 2008; accepted 13 February 2008

Available online 20 February 2008

Abstract

Previous acoustic instrumentation of the SIMPLE detector has relied on the use of a low-cost piezoelectric transducer, which was generally unable to provide discrimination between true bubble nucleation events and ambient sources of acoustic noise. The use of a high-quality electret microphone and adaptive electronics is shown to provide this capacity through reduced noise levels and distinct fast Fourier transforms of the event registration.

© 2008 Elsevier B.V. All rights reserved.

PACS: 43.58.+z; 29.40.-n; 95.35.+d

Keywords: Dark matter; Superheated liquids; Instrumentation; Signal discrimination

1. Introduction

The SIMPLE dark matter project [1] is based on superheated droplet detectors (SDDs), a suspension of micrometric superheated droplets inside a viscous elastic gel, which undergo transitions to the gas phase upon energy deposition by incident radiation: each droplet behaves as a miniature bubble chamber. It is one of only two such international dark matter searches (the other being PICASSO [2]) using high-concentration (1–3%) fluorine-based devices. Both have provided, with exposures of only 0.42 and 2 kg d respectively, constraints on the spin-dependent sector of the WIMP–nucleus interaction com-

parable with those of other, significantly larger exposure experiments [3].

The reasons for this competitiveness is the insensitivity of the SDDs to the majority of the backgrounds which plague the more traditional search activities (eliminating the need for sophisticated background discrimination techniques above the level of the intrinsic radio-impurities of the detector composition), and its fluorine content which provides the highest spin-dependent sensitivity available. This insensitivity derives from the response of SDDs [4]: if, within the metastable droplet, the energy deposition is (1) higher than a critical energy E_c , and (2) within a critical distance s ($dE/dx > E_c/s$), the droplet vaporizes. Both thresholds are thermodynamic, and can be selected by varying the operating pressure and temperature to render the SDD insensitive to energetic muons, gammas-rays, X-rays, electrons and other radiations depositing less than ~ 200 keV/ μm , i.e. the majority of traditional detector backgrounds which plague more conventional dark matter search detectors. This insensitivity is not trivial, amounting

*Corresponding author at: Instituto Tecnológico e Nuclear, Estrada Nacional 10, 2686-953 Sacavém, Portugal.

E-mail address: felizardo@itn.pt (M. Felizardo).

¹Present address: Department of Physics, University of Montreal, Montreal, Canada H3C 3J7.

²Present address: Department of Physics and Astronomy, University of New Mexico, Albuquerque, NM 87131, USA.

to an intrinsic rejection factor several orders of magnitude larger than the bolometer experiments with particle discrimination.

Low-concentration SDDs, being transparent, are read-out optically [5]. High-concentration devices are in contrast generally translucent, and both projects have adopted acoustic readout in instrumenting their detectors. The first SIMPLE data acquisition was based [6] on a piezoelectric transducer (PKM 13EPY-4002-Bo), although possessing a well-defined frequency response, the signal was accompanied by a relatively large (100 mV) noise level. In consequence, the device response was essentially that of a buzzer, and unable to discriminate true bubble nucleations from acoustic backgrounds such as microleaks arising from the escape of the overpressuring gas into the surrounding water bath [6], or fracturing of the gel with bubble growth during the device use. The inability to discriminate microleaks imposed a serious constraint on the previous SIMPLE measurements, since these accounted for the majority of the recorded events [1].

Recently, we reported the development of an improvement in the piezo-based acoustic instrumentation of the SDD [7], which yielded significantly reduced noise levels, permitting a form of discrimination between true signal and microleak events. The results indicated the possibility of a more complete acoustic background rejection with the use of a true microphone-based acquisition system. We here report the realization of such a system. Section 2 describes the electronics. Performance tests of the new instrumentation under a variety of operating conditions are presented in Section 3, with the discrimination capacity of the acoustic backgrounds described in Section 4. The

results are discussed in Section 5 and conclusions drawn in Section 6.

2. The front-end electronics

A Panasonic microphone cartridge (MCE-200) was selected to permit a fast Fourier transform (FFT)-based frequency decomposition of the nucleation signal in a 0.020–16 kHz (3 dB) range. Its specifications include [8] a signal-to-noise ratio of 58 dB and sensitivity of 7.9 mV/Pa at 1 kHz.

The microphone was supported with a Texas Instruments PGA2500, a digitally controlled, analog microphone preamplifier designed for use as a front-end for high-performance audio analog-to-digital converters [9]. Its characteristics include low noise, a wide dynamic gain range of 10–65 dB (1 dB/step), and low harmonic distortion. DC offset is minimized by an on-chip DC servo loop; common-mode rejection is increased via a common-mode servo function. The preamplifier is programmed using a 16-bit control word, loaded using a serial port interface. External switching of input pads, phantom power, high-pass filters, and polarity reversal functions are controlled via four programmable digital outputs. The main functions of the PGA2500 are shown in Fig. 1. Configurable input and output circuitry provide convenient prototype options, while the buffered host interface supports the supplied applications software and alternate host configurations.

The suggested basic circuit configuration [9] was initially employed, with phantom power disconnected but with both +5 and –5 V power supplies. Minor modifications of several capacitances and resistances were required in the

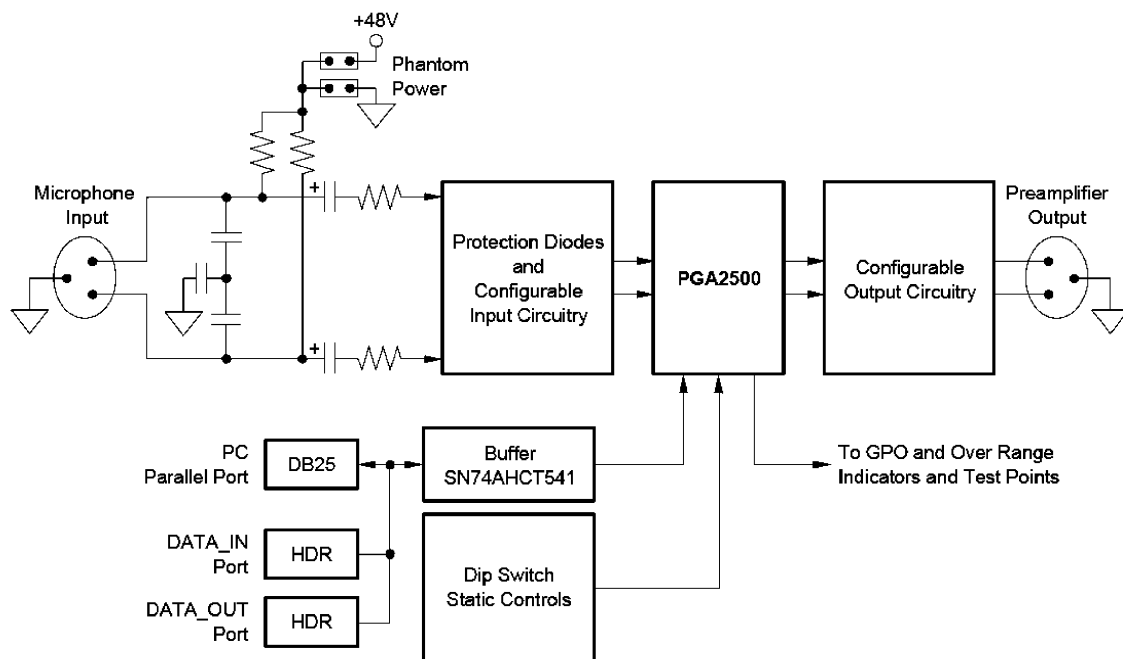


Fig. 1. Functional block diagram for the PGA2500EVM [9].

course of testing. During this testing, however, it was found that the voltage regulators made the circuit unstable, and that the protective diodes introduced noise into the system. In consequence, the configurable output circuitry was not

used; the final electrical circuit for the PGA2500/microphone system is shown in Fig. 2.

The circuit was assembled on a two-layer printed circuit board using both through-holes and surface-mount

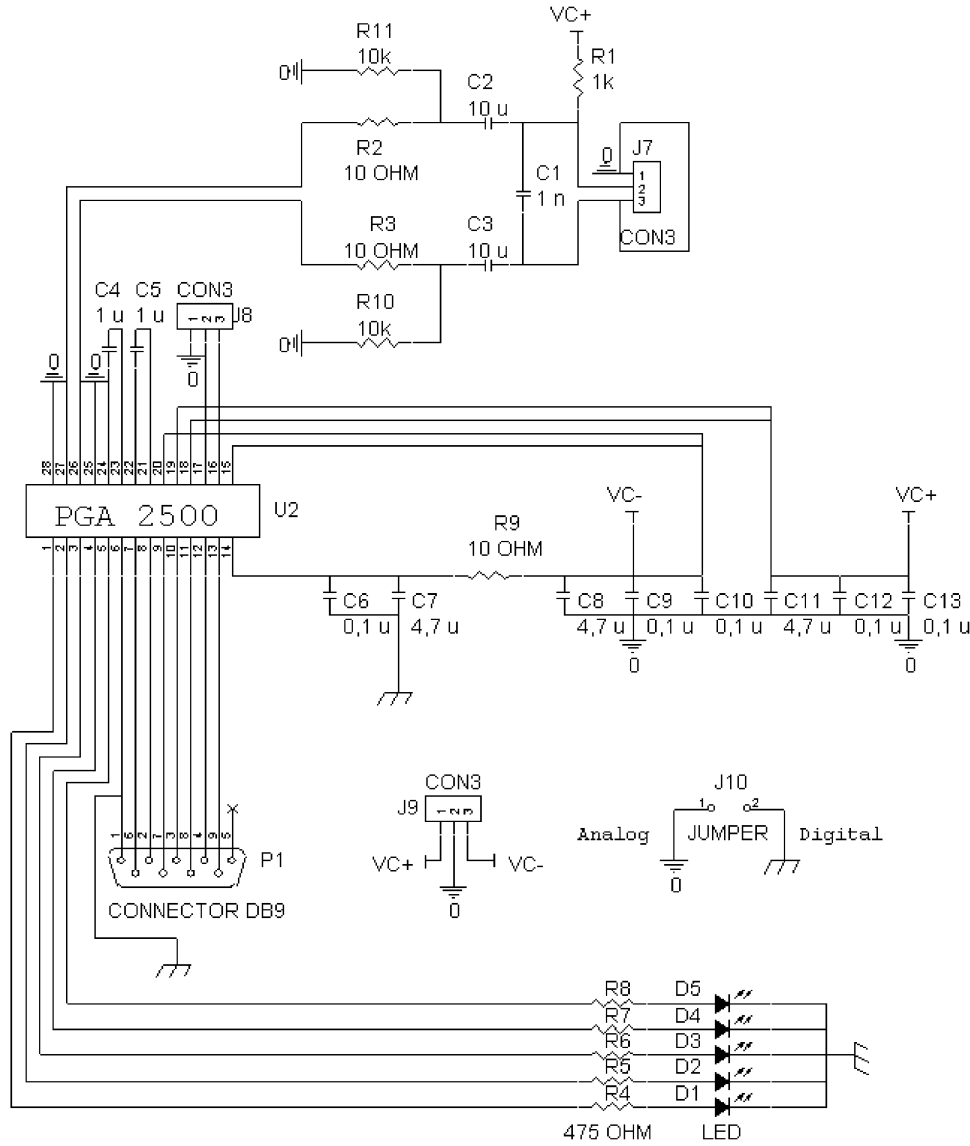


Fig. 2. Final electronic circuit for the PGA2500-microphone system.

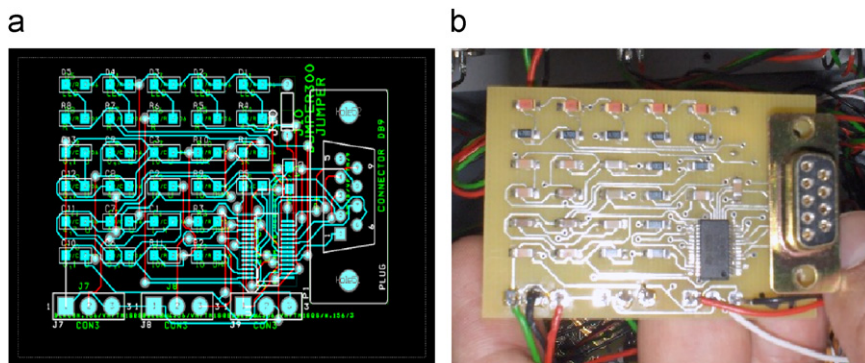


Fig. 3. Blueprint (a) and photo (b) of the assembled surface mount display electronics.

components. The top and bottom layer plots employed from the circuit of Fig. 2 are shown in Fig. 3.

3. Performance tests

3.1. Noise levels

Five boards were constructed according to the electronic circuit in Fig. 2 using standard components, and tested with respect to noise. As seen in Fig. 4, until 30 dB the noise level is ~1 mV, but the amplification is insufficient for the observation of a nucleation event. Between 40 and 60 dB, the choice was 60 dB, as the five boards had the best noise level among themselves (13.02 ± 0.19 mV). The maximum gain was rejected, since the ~400 mV noise level prevents a clear identification of nucleation events. No significant difference in performance was registered among the five boards.

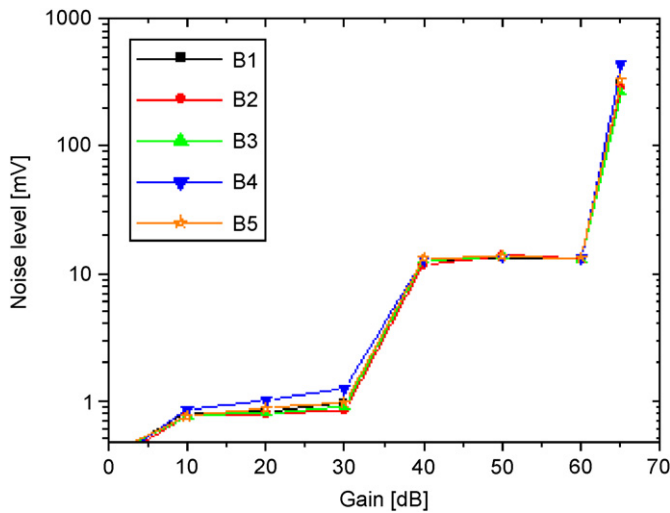


Fig. 4. Noise levels of the five amplifier boards.

3.2. Frequency response

All five boards were tested at zero gain with the microphone against a function generator, which as shown in Fig. 5(a) was set to produce a sine wave with amplitude of 1.5 V and a frequency of 3 kHz. All boards produced a well-defined peak around 3 kHz, as shown in Fig. 5(b).

3.3. Comparison with previous transducer

The new microphone-based instrumentation was also tested against the previous piezoelectric transducer system [7]. The intent was to compare the efficiency in counting events. For this, both transducer and microphone were set side by side in a water bath, through which N₂ gas was bubbled at a constant rate. The result is shown in Fig. 6; both systems recorded the same number of events,

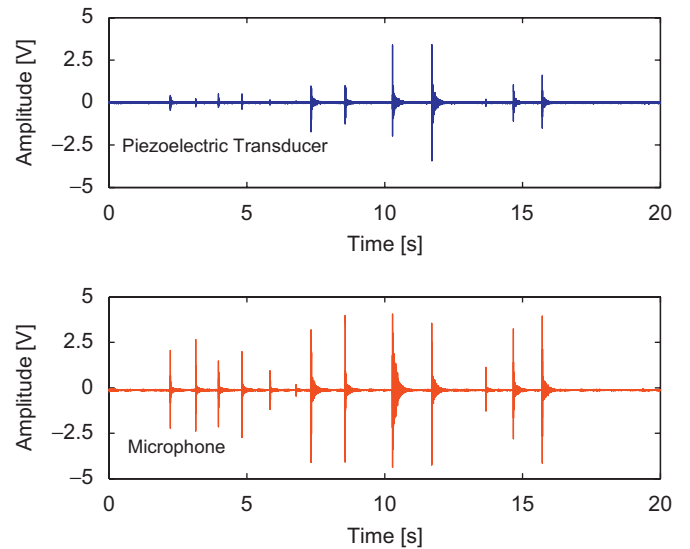


Fig. 6. Signal outputs for the piezoelectric (upper) and microphone (lower).

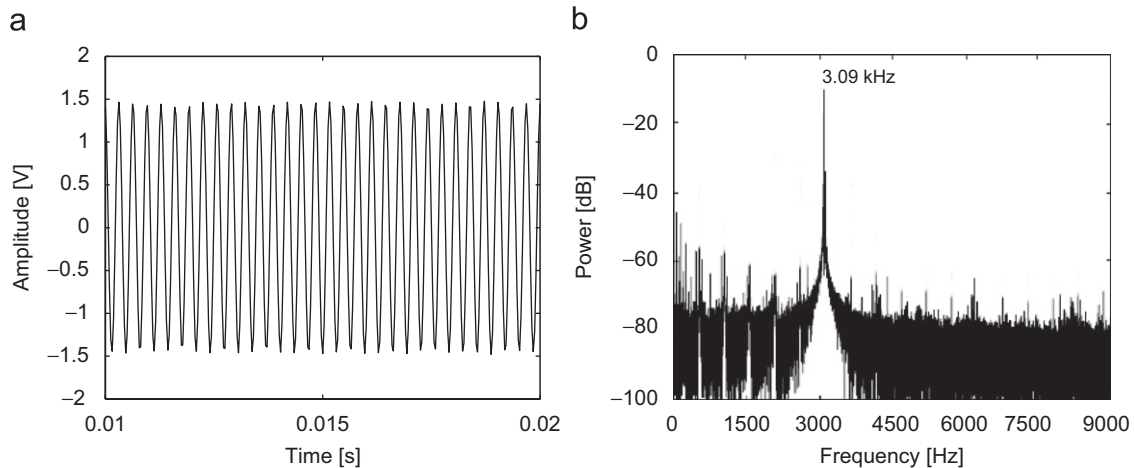


Fig. 5. (a) Signal output of the microphone + electronics against a 3 kHz function generator and (b) its FFT.

although the microphone signals show larger amplitudes and richer pulse structure.

3.4. Instrumentation robustness

A SIMPLE SDD is generally operated at temperatures and pressures which provide a minimum neutron recoil threshold energy while remaining below threshold for α 's, β 's and γ 's [5,6]. In the case of a standard C_2ClF_5 SIMPLE SDD, these are generally 2 bar at 9 °C. In general, pressure increase raises the threshold recoil energy curve and shifts it to higher temperatures, as shown in Fig. 7 for CCl_2F_2 . These thresholds depend on the critical temperatures of the

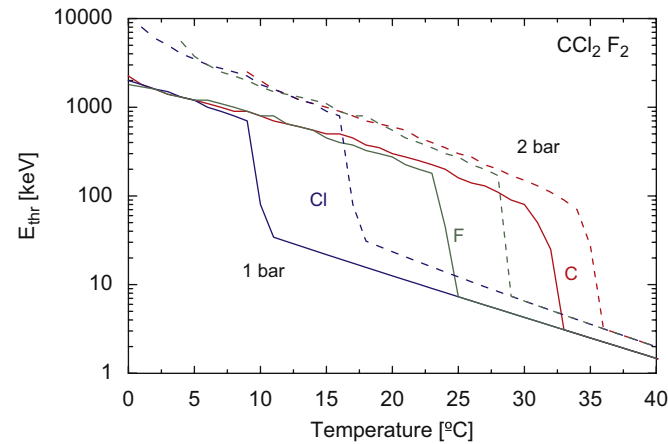


Fig. 7. Variation of threshold recoil energy curves for CCl_2F_2 with temperature, at 1 bar (solid) and 2 bar (dashed).

Table 1
Refrigerant critical temperatures [10] at 1 bar; T_b is the boiling temperature, T_c the critical

Temperature/refrigerant	C_2ClF_5	CCl_2F_2	C_4F_{10}	C_3F_8
T_b (°C)	-39.17	-29.76	-2.09	-36.65
T_c (°C)	79.9	111.8	113.18	71.95

refrigerant, which as seen in Table 1 vary significantly between the materials: different devices may be operated at higher temperatures or pressures, both of which may have adverse mechanical effects on the microphone.

Fig. 8 shows a typical bubble nucleation event and its FFT obtained with the new instrumentation, from a small volume prototype CCl_2F_2 SDD warmed to stimulate bubble nucleations. The FFT is characterized by a peak at ~ 640 Hz, with some lower power harmonics around 2 and 4 kHz. These events were cross-checked against nucleation events generated by irradiating the detectors using a quasi-monochromatic 54 keV neutron beam obtained with a Si+S passive filter at the Portuguese Research Reactor [11].

As a first-stage discrimination filter for distinguishing true nucleation events from acoustic backgrounds, the pulse shape validation routine developed for the previous instrumentation [7] was adopted. This routine:

- (i) sets an amplitude threshold;
- (ii) identifies the beginning and end of each spike, based on the previous threshold;
- (iii) amplitude demodulates the time evolution of the spike;
- (iv) measures the decay time constant (τ) of the pulse; and
- (v) suppresses the pulses which exhibit τ 's below a given threshold.

The choice of the amplitude threshold is an interactive procedure, and can be set very low for the rejection of spurious noise. Amplitude demodulation is achieved simply with the modulus of the Hilbert transform of the pulse waveform, $y(t) = |H\{x(t)\}|$. After the amplitude envelope has been obtained, the maximum and the minimum of the pulse shape are found to set the time window used for evaluating τ . The decaying part of the envelope is then fit to an exponential, $h(t) = A e^{-t/\tau}$, by means of a linear regression after linearizing the envelope, $\ln(y(t)) = \ln(A) - t/\tau + \text{er}(t)$ where $\text{er}(t)$ corresponds to the residual of the fit. Fig. 9 shows both the decay interval of

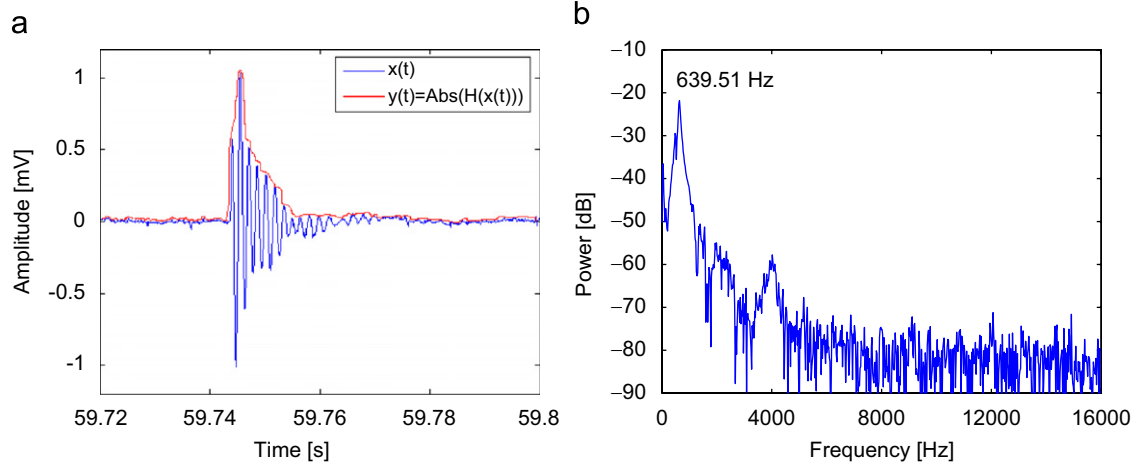


Fig. 8. Typical pulse shape (a) and FFT (b) of a bubble nucleation event.

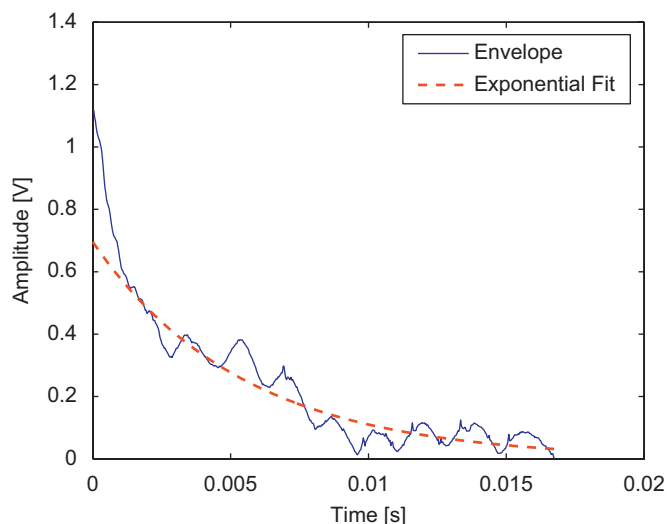


Fig. 9. Best fit to an exponential function of the amplitude envelope from the pulse shown in Fig. 8, with $\tau \sim 20$ ms.

the envelope, and the exponential fit. An efficiency of 100% was obtained with a τ window of 10–40 ms.

3.4.1. Temperature variations

A standard detector (2.5 g of CCl_2F_2), at 1 bar pressurization, was ramped in temperature between 15 (~ 20 keV recoil threshold) and 35°C , the latter set by SIMPLE's use of food gels for which melting begins. Given the (T , P)-dependent SDD threshold, the sensitivity varied over the experiments: for 35°C , the reduced superheat factor [5] for CCl_2F_2 is 0.46, slightly below the $s = 0.5$ threshold for β , γ and μ sensitivity [5,11], and the device was generally sensitive to only environmental neutrons. Fig. 10(a) and (b) displays the variation of noise level and recorded events, respectively, with detector temperature, normalized with respect to detector freon mass. Within experimental uncertainties, the noise level was basically independent of temperature. The number of nucleations increases abruptly above 20°C , corresponding [5] to a minimum incident neutron energy of ~ 150 keV (~ 10 keV in recoil), as shown in Fig. 10(b). Although usually indicative of a threshold crossing, the CCl_2F_2 is generally insensitive to minimum ionizing radiation below $\sim 41^\circ\text{C}$ [5].

Fig. 10(c) and (d) similarly displays the variation with temperature of the signal amplitude and time constant, respectively. The amplitudes generally remain unchanged until the gel medium enters the pre-melting phase at 35°C , and the large increase is likely the result of multiple events coincident in time. The time constants indicate approximately factor 2 variation over the temperature range, which surprisingly is parabolic with maximum in the midrange temperature.

The variation of the frequency response with temperature is shown in Fig. 10(e), which also exhibits a parabolic behavior with minimum at about the same temperature as the maximum of the signal time constants. Only a single principal frequency ranging between 400 and 800 Hz is observed at each temperature.

3.4.2. Pressure variations

The SIMPLE C_2ClF_5 SDDs are generally operated at 2 bar in order to increase their insensitivity to common background radiations; they have been over-pressured to as much as 4 bar for transportation without damage to the construction. Since the CCl_2F_2 SDD sensitivity at higher pressures is shifted nearer the 35°C gel melting temperature (see Fig. 7), SDDs based on C_3F_8 were utilized for which the sensitivity is essentially the same in the 10– 35°C range. The response of a standard (3.1 g) SDD at 2 bar is shown below in comparison with a similar C_3F_8 device at 1 bar. The 2 bar device suffered a gel meltdown at 30°C .

The temperature variation of the noise levels and recorded events are shown in Fig. 11(a) and (b), respectively. The noise level is essentially unchanged with temperature increase, rising only slightly as the gel melting temperature is approached and remaining identical with the 2 bar device.

The number of nucleation signals (see Fig. 11(b)) at 2 bar in the temperature midrange is $\sim 4 \times$ less than at 1 bar, with the 2 bar results shifted to higher temperatures as anticipated. This is consistent with the signal amplitudes shown in Fig. 11(c), which at 2 bar are significantly lower than those at 1 bar, and most likely result from the compression of the microphone's diaphragm. In contrast, the time constants (see Fig. 11(d)) are essentially independent of the device pressuring, and show no evidence of parabolic variation with temperature at either pressure.

Fig. 11(e) shows the recorded signal frequencies for both devices. The 1 bar results are reasonably uniform and about equal to those of the CCl_2F_2 device at 25°C and 1 bar. At 2 bar, the frequency is a factor 2–3 higher than at 1 bar, consistent with the compression of the gel and stiffening of the propagation medium. In all cases, microphone performance characteristics at 1 bar were restored following the 2 bar tests, indicating no physical damage to the microphone functioning at the elevated pressure.

3.4.3. Glycerin layer

The previous instrumentation design mounted the transducer in a glycerin layer above the gel/refrigerant, shielded from direct contact by a latex sheath, in principle to amplify the transmitted acoustic wave from the gel [7]. The influence of the glycerin layer on a similarly mounted microphone performance was examined using two almost identical (2.5 and 3.2 g), standard (150 ml), CCl_2F_2 (2.5 g) SDDs, one without the glycerin layer. The devices were mounted in a water bath, as in the tests of Section 3.4.1.

The temperature variations of the noise and recorded events, normalized to freon mass, are shown in Fig. 12(a) and (b), respectively. The noise levels are basically the same in both detectors, and flat with temperature, although the noise level is slightly less in the detector without the glycerin layer. As seen in Fig. 12(b), the number of nucleation signals for the standard SDD increases with increasing temperature; without the glycerin layer, the

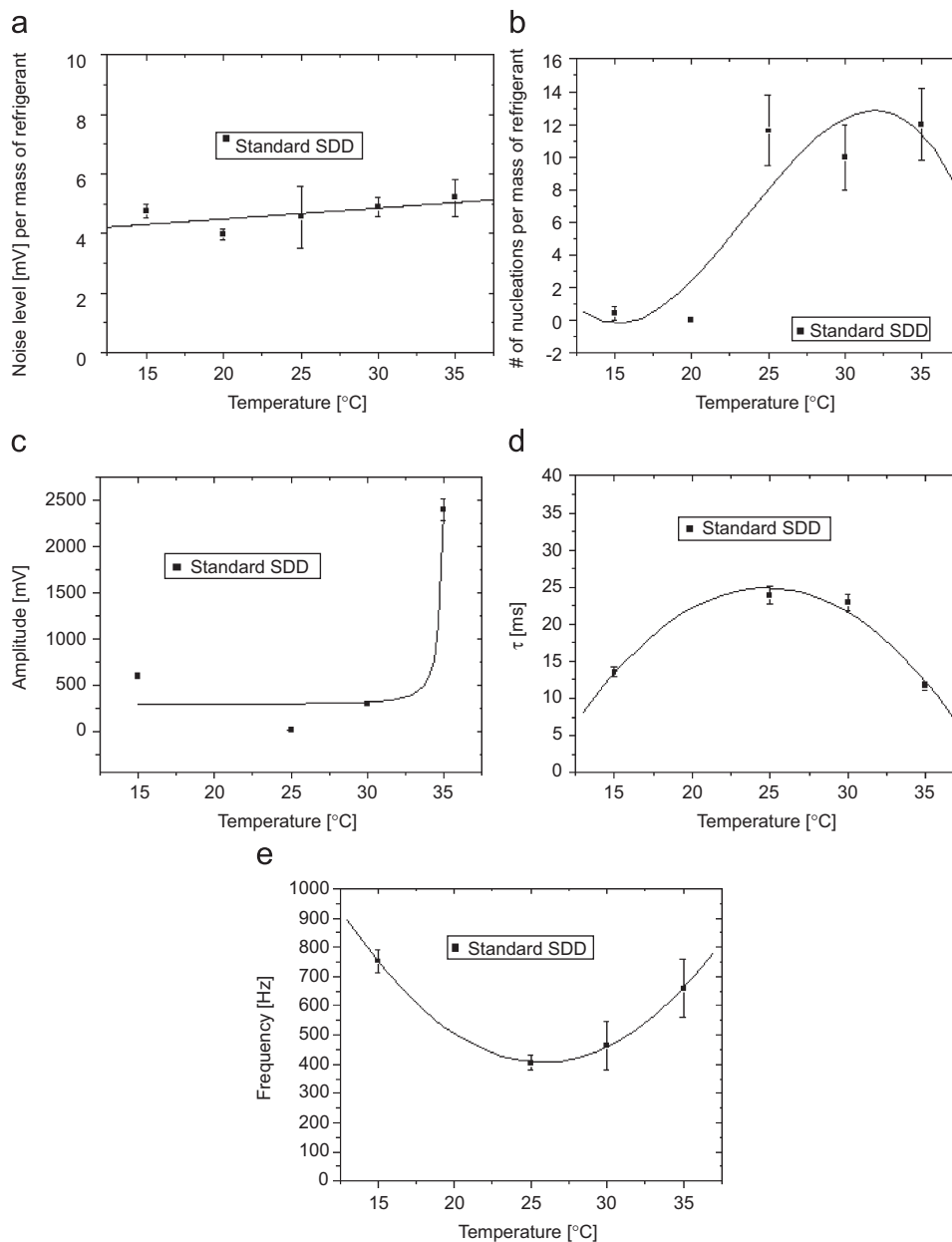


Fig. 10. Variation of signal (a) noise level, (b) event number, (c) amplitude, (d) time constant, and (e) frequency with temperature, for a CCl₂F₂ SDD at 1 bar pressure.

microphone is in air and fails to record the majority of the nucleation events—which were confirmed visually afterwards.

This is further evidenced in the temperature variations of the signal amplitudes and time constants of Fig. 12(c) and (d), respectively. Except at the highest temperature, the few nucleation signals from the “no glycerin layer” detector have amplitudes that are consistent with the standard SDD. The associated time constants are however essentially the same for both.

Fig. 12(e) shows the frequency variation of the two detector outputs with temperature. Apart from the one 1.5 kHz nucleation signal at 20 °C, the detector without the glycerin layer generally produced signals with frequencies

around 30 Hz, in contrast to the standard SDD response with frequencies in the vicinity of 600 Hz.

4. Acoustic background discrimination

The goal of a SDD instrumentation, apart from registration of true nucleation events, is a capacity to discriminate these events from a variety of general acoustic backgrounds common to SDD operation, which in an underground, low-background environment constitute a significant contribution to the event record. The pulse shape validation routine was again employed as a first-stage filter, in order to reduce the number of FFTs required in the signal analysis.

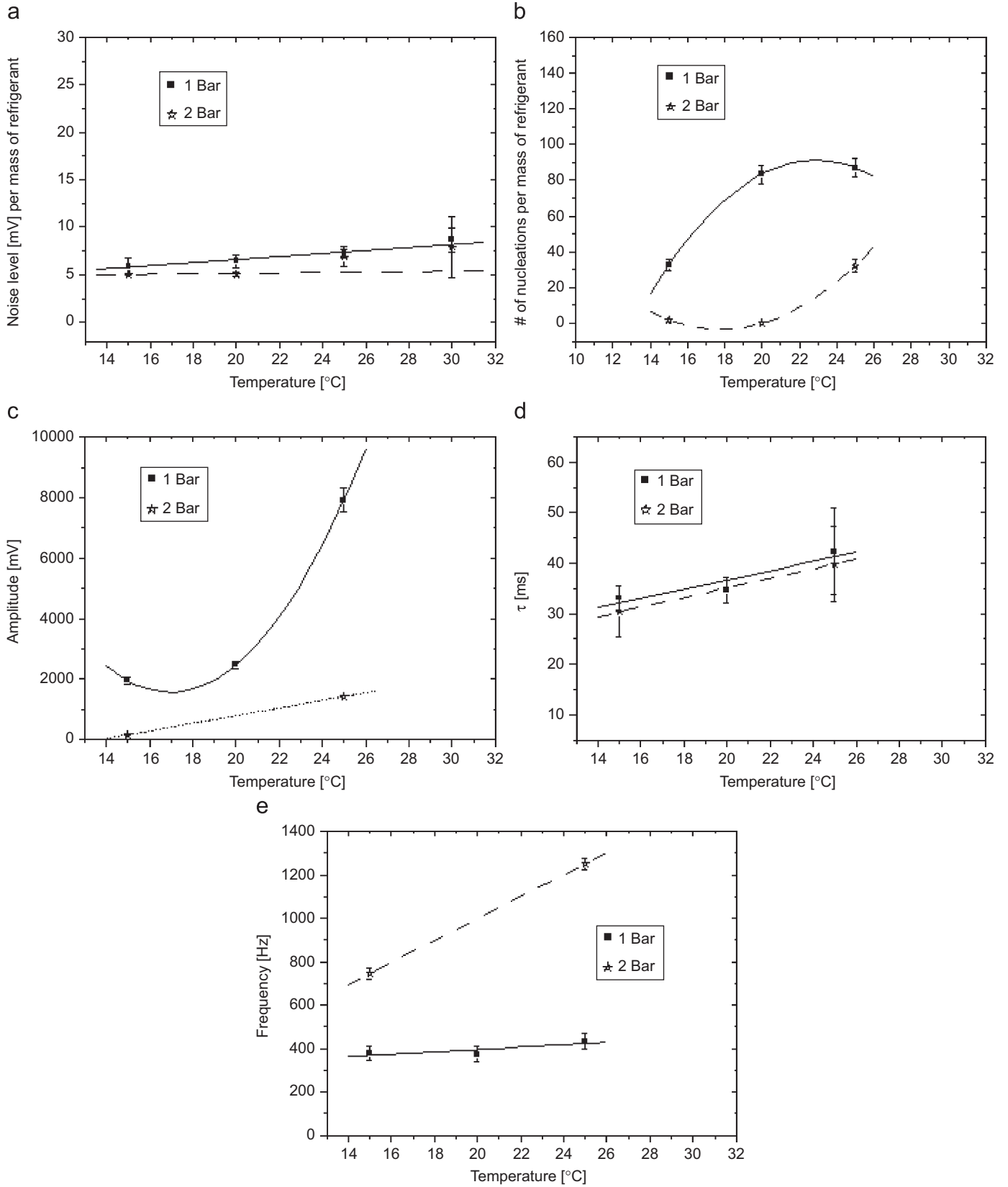


Fig. 11. Variation of signal (a) noise level, (b) event number, (c) amplitude, (d) time constant, and (e) frequency of C_3F_8 SDDs at 1 and 2 bar.

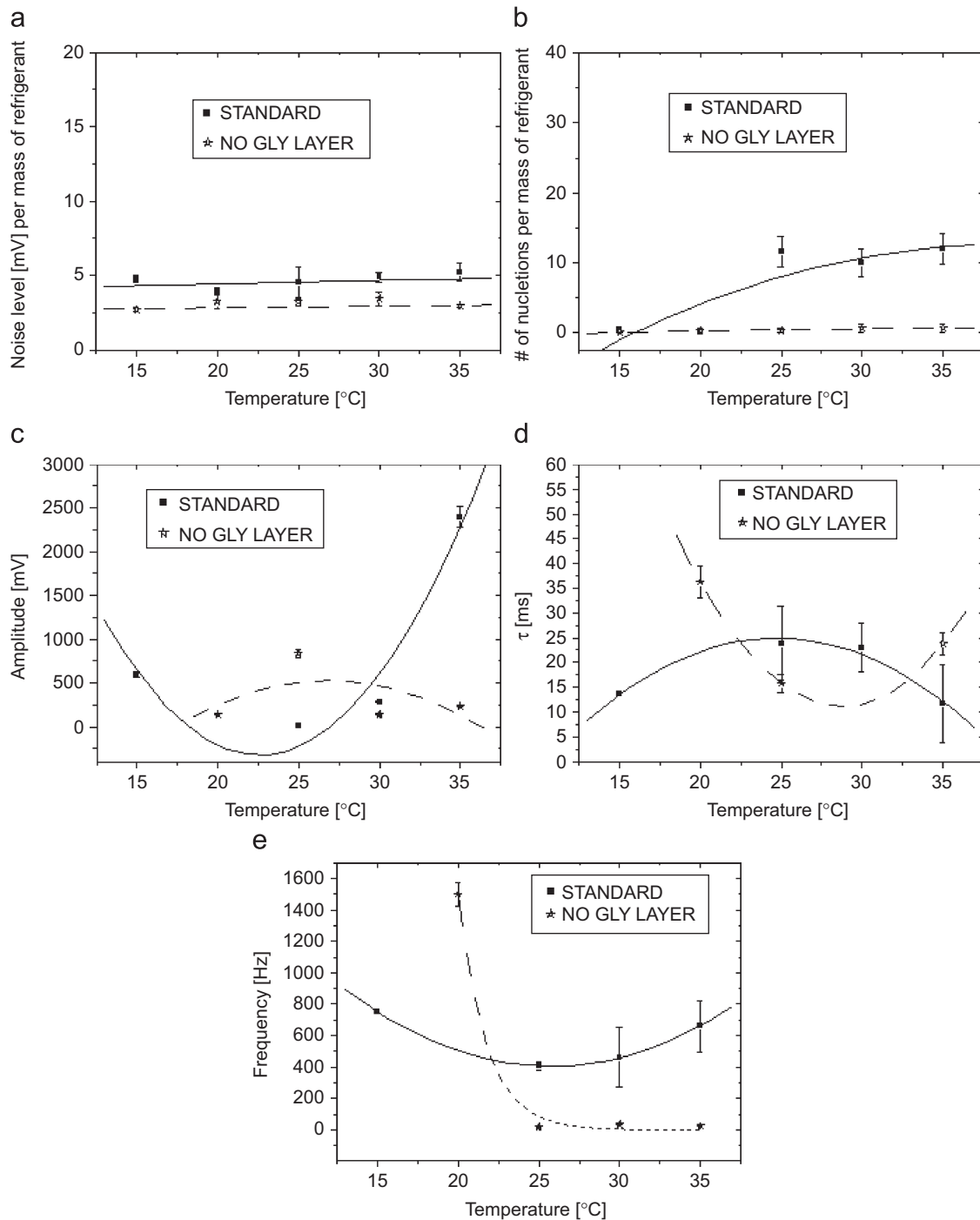


Fig. 12. Variation in signal (a) noise level, (b) event rate, (c) amplitude, (d) time constant, and (e) frequency for CCl_2F_2 detectors with and without the glycerin layer.

4.1. Microleaks

Pressure microleaks were forced by simply not fully tightening the new capping mechanism on a freon-less device. The result is shown in Fig. 13(a), where a large number of water bubbles from the bath container of the SDD is observed. If one of these spikes is isolated and enlarged, one can see that the pulse shape is not much

different from a true bubble nucleation (see Fig. 13(b)), consistent with previous observations [6].

The recorded signal satisfies the pulse validation filter as for true bubble nucleations, with $\tau = 17.2$ ms; its FFT is however observed to vary in frequency from 2.8 to 3.5 kHz, consistent with a dependence on the microleak size and release pressure. For this particular case, the pulse of Fig. 13(b) exhibits a principal frequency of 3.44 kHz

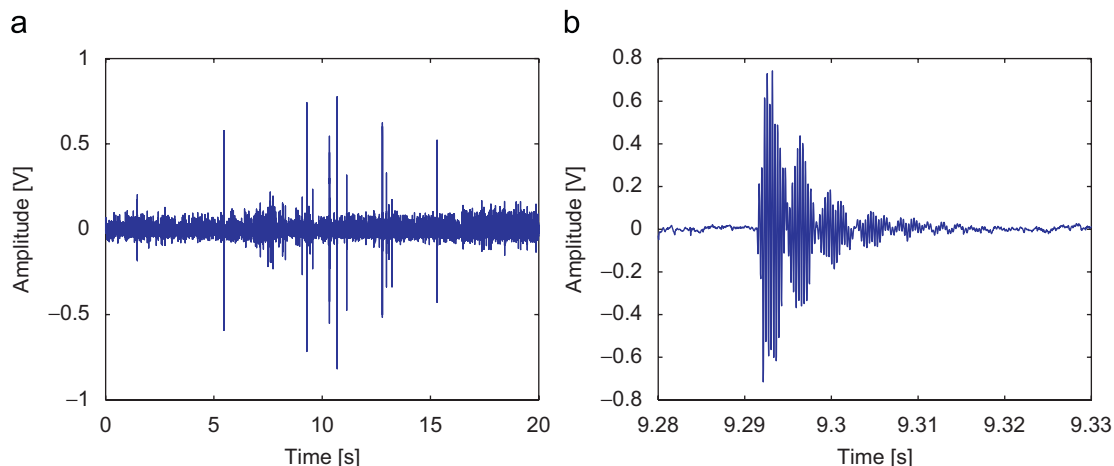


Fig. 13. (a) Signal with forced microleaks and (b) zoom of one of the spikes in (a).

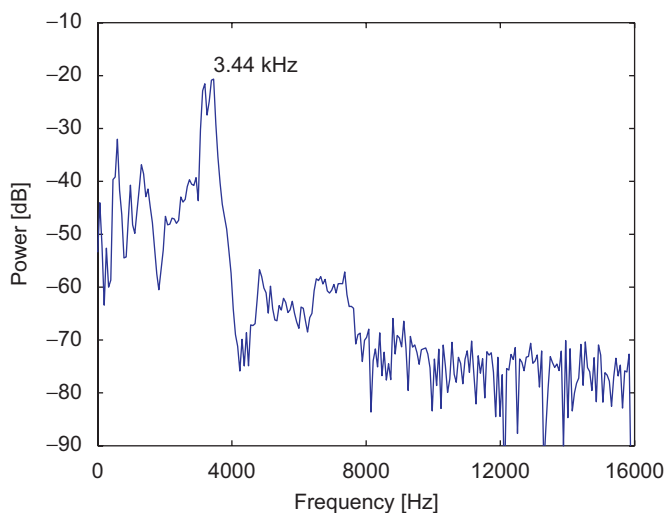


Fig. 14. FFT of a microleak registered by the microphone.

(see Fig. 14) at about the same power level as a true nucleation event, but with a spectrum clearly distinguishable from Fig. 8(b).

4.2. Fractures

On occasion, SDDs exhibit fractures caused by deterioration of the gel (such as with an old detector), or by the nucleation of large droplets that trigger the nucleation of their surrounding neighbors. This was examined with the new instrumentation using SDDs which had been refrigerated at -36°C for over 4 years, and several more recent fabrications in which gel fracturing was deliberately enhanced using more soluble refrigerants such as CF_3I . As shown in Fig. 15(a), when a fracture occurs, only one event is generally recorded; the majority of these again satisfied the pulse shape validation routine, with τ 's ~ 36.4 ms. As seen in Fig. 15(b), the FFT of the entire fracture however indicates most of the power is in ~ 34.37 Hz with several harmonics at ~ 400 Hz intervals,

and a spectrum clearly distinguishable from a true nucleation event.

4.3. Trapped N_2 gas

Some nitrogen gas may remain trapped inside the gel after the SDD production at 20 bar in the hyperbaric chamber, and then be released to produce a signal once at normal atmosphere conditions. A test was conducted using a “refrigerant-less SDD”, with no overpressure in order to avoid microleaks.

Measurements were performed immediately within the first hour after the “detector” was removed from the hyperbaric chamber. This time, the event shown in Fig. 16(a) did not satisfy the pulse shape identification routine due to its large $\tau = 90.9$ ms; its FFT shown in Fig. 16(b) is furthermore clearly peaked at ~ 40 Hz with a power level $\sim 50\%$ of a true nucleation, and manifests a strongly different spectrum.

5. Discussion

Performance testing of the new instrumentation demonstrates better than a factor 10 reduction in noise compared with the previous transducer instrumentation, with signal amplitudes increased by factors of 2–10 ($S/N \sim 10$). The parabolic behavior of the variation of the signal amplitude, time constant and frequency with temperature at 1 bar pressuring is unexpected. With increasing temperature, the gel becomes less stiff, and decreasing frequencies and larger signal time constants could easily be expected; why these trends should reverse themselves as the gel approaches a melting phase is not at all yet understood, and require further study.

The overall results of the background discrimination tests are shown in Table 2. The results clearly demonstrate the capacity of the microphone-based instrumentation to distinguish internal acoustic backgrounds commonly associated with SDD operation. The principal frequency

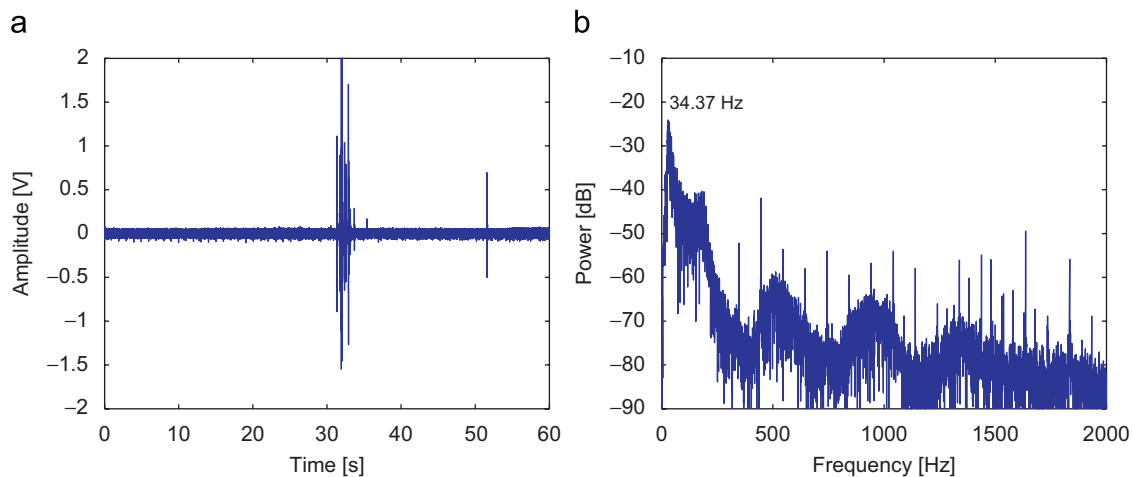


Fig. 15. (a) Signal of a fracture in the gel of a SDD and (b) frequency spectrum of the fracture shown in (a).

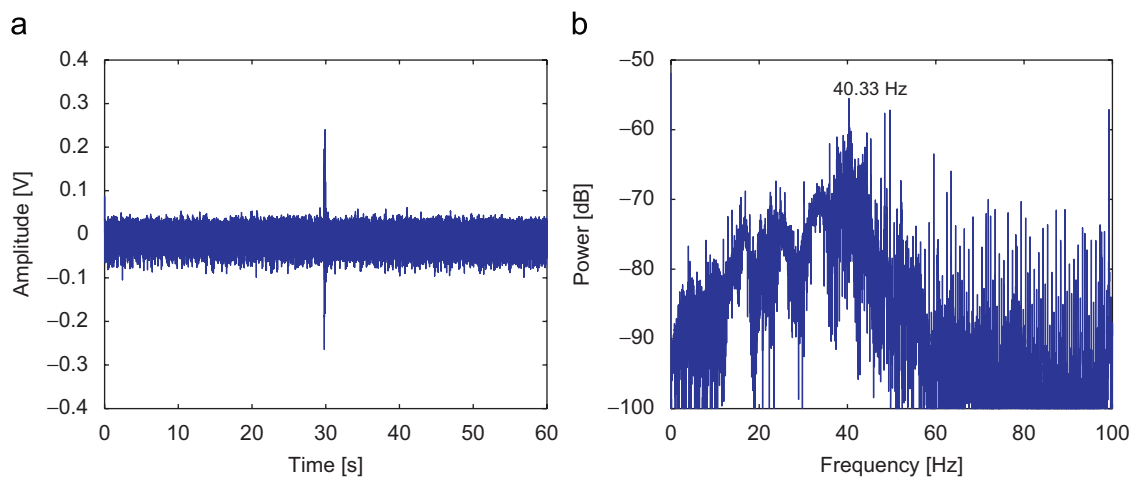


Fig. 16. Typical (a) nitrogen release event from the gel and (b) FFT of the event in (a).

Table 2
Comparison of true event characteristics from a CCl_2F_2 SDD with those of several common acoustic backgrounds

Event type	Time constant (ms)	Principal frequency (Hz)	Power level (dB)
True nucleation	20.1	640	-20 ± 6
Microleak	17.2	2800–3500	-25 ± 10
Fracture	36.4	34	-25 ± 8
Trapped N_2	90.9	40	-55 ± 3

associated with each of the acoustic backgrounds presented is clearly different from a true bubble nucleation event. Most of these background events pass the first-stage filter (pulse shape routine), the trapped N_2 being the exception. Conversely, the FFTs of a random selection of the signals eliminated by the validation routine correspond to none of the event types of Table 2. Although the actual discrimination is effected on the basis of the FFT, the pulse shape validation routine serves to reduce the number of events to be processed.

Occasionally, some events were recorded with significantly distinct and higher frequencies. Although not specifically part of this study, true nucleation event results from a CF_3I study were additionally filtered through low pass (0–5 kHz), bandpass (5–10 kHz) and high-pass (10–16 kHz) filters. When one of the largest amplitude spikes is expanded (see Fig. 17(a)), there is no record of a signal in the high-frequency range. The individual FFTs are shown in Fig. 17(b). The band pass filter shows a lower power plateau of higher frequency, but with amplitude ~ 0.15 V compared with ~ 1 V of the actual bubble nucleation.

Higher frequency signals are in fact anticipated from the theory of the formation of a gas bubble by a particle passing through a superheated droplet detector [2,12], which suggests that the process can be split into four stages in time [12]:

- (i) interaction of a charged particle with the liquid atoms;
- (ii) the transition of energy, heating the region around the particle track;
- (iii) the emergence of a gaseous phase nucleus; and
- (iv) growth of the gas nuclei.

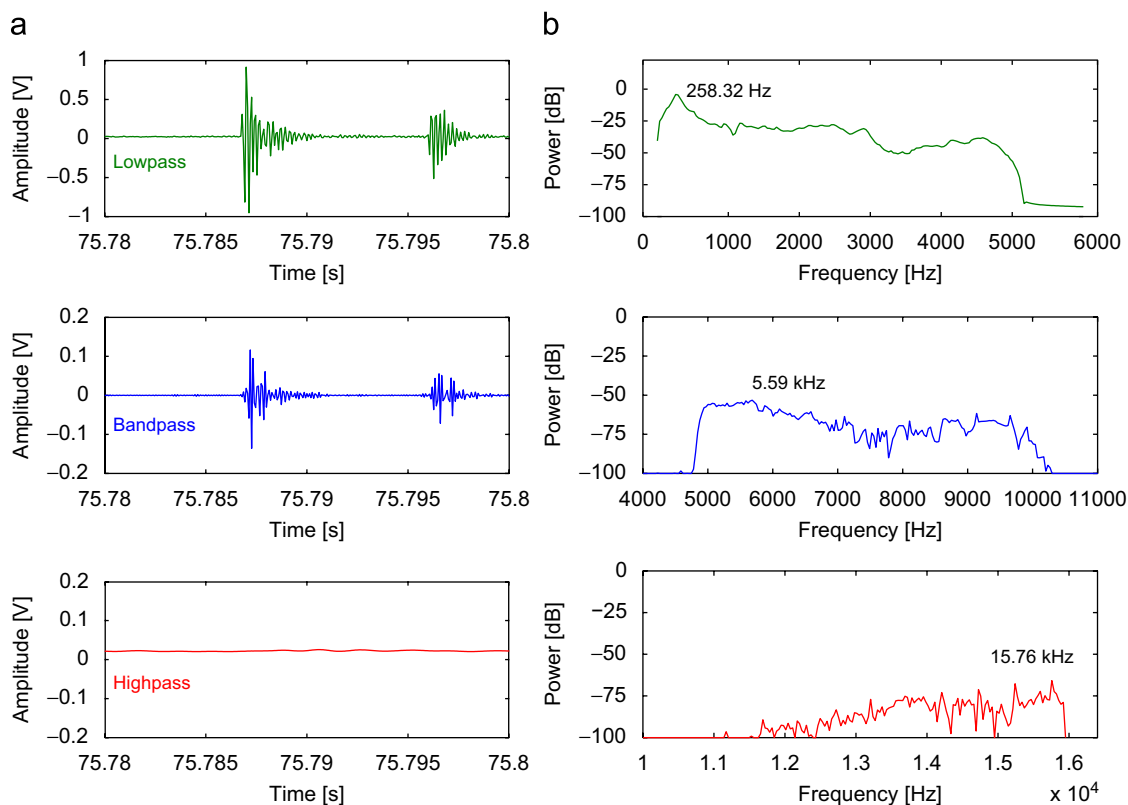


Fig. 17. (a) Filtered SDD signal data showing evidence of frequency components associated with the same bubble nucleation and (b) FFTs of the three frequency filters of the true nucleation event in (a).

The acoustic signal currently detected by the instrumentation derives from the last stage, which is essentially independent of the event origin. The preceding stage, in which the nucleus of the gas phase emerges, however, in principle however depends on the origin of the energy deposition, which in turn depends on the nature of the incident particle. Identification of this nucleation stage would provide a crucial improvement in the SDD discrimination capacity. If the nanosecond time scales estimates [12] of the fourth stage are however accurate, ultrasonic instrumentation is likely required, and remains to be explored.

The new instrumentation is currently undergoing testing in the electromagnetically shielded underground laboratory of the Laboratoire Souterrain Bas Bruit de Rustrel (LSBB), which is also the site of the SIMPLE experiment [13]. Preliminary results indicate performances identical to those of the surface tests reported here, but with a noise level reduced by approximately 50%.

6. Conclusions

An efficient and low noise instrumentation based on a high-quality electret (MCE-200) microphone has been designed and built. The performance demonstrates better than a factor 10 reduction in noise compared with the previous transducer instrumentation, with signal amplitudes increased a factor 2–10. No significant variation in

the instrumentation response was observed in testing at different temperatures and pressures, beyond signal frequency shifts that may be related to the gel as its melting temperature is approached. The use of a glycerin layer surrounding the microphone and above the SDD is shown to provide a superior response.

The low noise and higher signal amplitudes of the new instrumentation permits a capability of discriminating nucleation events from acoustic backgrounds common to SDDs, including microleaks, fractures and trapped nitrogen gas. The next step is the discrimination of the radiations initiating the nucleation events, for which ultrasound techniques will be required. Also in progress is the spatial localization of the events using multiple microphone arrays, which should permit rejection of α -particle events originating at the detector walls.

Acknowledgments

We thank the Portuguese Research Reactor crew for their contributions to these measurements. The work of M. Felizardo was supported by POCI grant FIS/55930/2004 of the Portuguese Foundation for Science and Technology (FCT); T. Morlat by POCI grant FIS/57834/2004; F. Giuliani by grant SFRH/BPD/13995/2003 of FCT. The activity was also supported in part by POCI grant FP/63407/2005 of FCT, co-financed by FEDER.

References

- [1] T.A. Girard, F. Giuliani, J.I. Collar, D. Limagne, H.S. Miley, T. Morlat, G. Waysand, M. Auguste, D. Boyer, A. Cavallou, J.G. Marques, C. Oliveira, J. Puibasset, M. da Costa, A.C. Fernandes, A.R. Ramos, R.C. Martins, *Phys. Lett. B* 621 (2005) 233.
- [2] M. Barnabé-Heider, M. Di Marco, P. Doane, M.-H. Genest, R. Gornea, R. Guénette, C. Leroy, L. Lessard, J.-P. Martin, U. Wichoski, V. Zacek, K. Clark, C. Krauss, A. Noble, E. Behnke, W. Feighery, I. Levine, C. Muthusi, S. Kanagalingam, R. Noulty, *Phys. Lett. B* 624 (2005) 186.
- [3] F. Giuliani, T.A. Girard, *Phys. Rev. D* 71 (2005) 123503.
- [4] F. Seitz, *Phys. Fluids* 1 (1958) 2.
- [5] F. d'Errico, *Nucl. Instr. and Meth. B* 184 (2001) 229.
- [6] J.I. Collar, J. Puibasset, T.A. Girard, D. Limagne, H.S. Miley, G. Waysand, *New J. Phys.* 2 (2000) 14.1.
- [7] M. Felizardo, R.C. Martins, T.A. Girard, et al., *Nucl. Instr. and Meth. A*, 2007, doi:10.1016/j.nima.2007.11.018.
- [8] Panasonic MCE-200 Data Specs <<http://monacor.no/go/?p=MCE-200>>.
- [9] Texas Instruments PGA2500 Data Specs <<http://www.ti.com/>>.
- [10] F. d'Errico, M. Matzke, *Radiat. Protect. Dosim.* 107 (2003) 111.
- [11] F. Giuliani, C. Oliveira, J.I. Collar, et al., *Nucl. Instr. and Meth. A* 526 (2004) 348.
- [12] Yu.N. Martynyuk, N.S. Smirnova, *Sov. Phys. Acoust.* 27 (1991) 376.
- [13] Laboratoire Souterrain à Bas Bruit de Rustrel-Pays d'Apt <<http://lsbb.unice.fr>>.